PLOS ONE

RESEARCH ARTICLE

Overexpression of oncogenic H-Ras in hTERT-immortalized and SV40-transformed human cells targets replicative and specialized DNA polymerases for depletion

Wei-chung Tsao[1], Raquel Buj[2¤], Katherine M. Aird[2,3¤], Julia M. Sidorova[4], Kristin A. Eckert[1,3]*

1 Department of Pathology, The Jake Gittlen Laboratories for Cancer Research, Penn State University College of Medicine, Hershey, Pennsylvania, United States of America, **2** Department of Cellular and Molecular Physiology, Penn State University College of Medicine, Hershey, Pennsylvania, United States of America, **3** Penn State Cancer Institute, Pennsylvania State University, Hershey, Pennsylvania, United States of America, **4** Department of Pathology, University of Washington, Seattle, Washington, United States of America

¤ Current address: Department of Pharmacology & Chemical Biology, UPMC Hillman Cancer Center, University of Pittsburgh School of Medicine, Pittsburgh, Pennsylvania, United States of America
* kae4@psu.edu

OPEN ACCESS

Citation: Tsao W-c, Buj R, Aird KM, Sidorova JM, Eckert KA (2021) Overexpression of oncogenic H-Ras in hTERT-immortalized and SV40-transformed human cells targets replicative and specialized DNA polymerases for depletion. PLoS ONE 16(5): e0251188. https://doi.org/10.1371/journal.pone.0251188

Editor: Anja-Katrin Bielinsky, University of Minnesota Twin Cities, UNITED STATES

Received: February 9, 2021

Accepted: April 21, 2021

Published: May 7, 2021

Data Availability Statement: All relevant data are within the paper and its Supporting information files.

Funding: This study was supported by the National Institutes of Health (R01CA237153 to K.A.E., R00CA194309, R37CA240625 to K.M.A., R01GM115482 to J.M.S), by the Pennsylvania Department of Health SAP # 4100083097 (to K.M. A. and K.A.E.), by the Penn State Cancer Institute (Postdoctoral Fellowship to R.B.), and by the Jake

Abstract

DNA polymerases play essential functions in replication fork progression and genome maintenance. DNA lesions and drug-induced replication stress result in up-regulation and re-localization of specialized DNA polymerases η and κ. Although oncogene activation significantly alters DNA replication dynamics, causing replication stress and genome instability, little is known about DNA polymerase expression and regulation in response to oncogene activation. Here, we investigated the consequences of mutant *H-RAS*^{G12V} overexpression on the regulation of DNA polymerases in h-*TERT* immortalized and SV40-transformed human cells. Focusing on DNA polymerases associated with the replication fork, we demonstrate that DNA polymerases are depleted in a temporal manner in response to *H-RAS*^{G12V} overexpression. The polymerases targeted for depletion, as cells display markers of senescence, include the Pol α catalytic subunit (*POLA1*), Pol δ catalytic and p68 subunits (*POLD1* and *POLD3*), Pol η, and Pol κ. Both transcriptional and post-transcriptional mechanisms mediate this response. Pol η (*POLH*) depletion is sufficient to induce a senescence-like growth arrest in human foreskin fibroblast BJ5a cells, and is associated with decreased Pol α expression. Using an SV-40 transformed cell model, we observed cell cycle checkpoint signaling differences in cells with H-Ras^{G12V}-induced polymerase depletion, as compared to Pol η-deficient cells. Our findings contribute to our understanding of cellular events following oncogene activation and cellular transformation.

Introduction

DNA replication is a critical phase of the cell cycle that must be tightly regulated to ensure accurate genome duplication. Failure to maintain DNA replication regulation leads to genome

Gittlen Laboratories for Cancer Research. The funders had no role in study design, data collection and analysis, decision to publish, or preparation of the manuscript.

Competing interests: The authors have declared that no competing interests exist.

instability and ultimately tumorigenesis. Activating mutations in oncogenes alter DNA replication dynamics, promoting replication stress and genome instability [1, 2]. In turn, cells can undergo proliferative arrest known as oncogene-induced senescence, which acts as a tumorigenic barrier by preventing neoplastic transformation [1–4]. Replication stress is broadly defined as the slowing or stalling of the replication fork when the replisome encounters obstacles during DNA replication, and is associated with genome instability [5]. The replisome is a highly dynamic structure that incorporates multiple DNA polymerases, enzymes that are integral to all replication processes, including ongoing fork elongation, fork restart, and fork repair [6–10]. The regulation of various DNA polymerases to accomplish replication in response to exogenous, DNA damage-induced replication stress has been well studied [11, 12]. Critically, less is understood about the impact of oncogene-induced DNA damage on DNA polymerase regulation.

Significant evidence supports the hypothesis that the replication stress and DNA damage responses are induced during oncogene activation, prior to senescence [1, 13, 14]. Oncogenic Ras activation causes replicative stress, DNA damage, and senescence through a variety of mechanisms [1, 2, 15, 16]. Constitutively activated mutant *H-RAS* (hereafter referred to as Ras^{G12V}) increases CDK2 activity and subsequent G1/S checkpoint abrogation, leading to increased origin firing, hyper-replication, and aberrant cell proliferation [1, 17]. Consequently, the prolonged presence of Ras^{G12V} activity is thought to cause replication stress through increased production of reactive oxygen species, replication-transcription machinery collisions, and depleted dNTP pools [16, 18–22].

The fidelity of genome replication is orchestrated by engaging multiple DNA polymerases [23]. Replicative polymerases delta (Pol δ) and epsilon (Pol ε) replicate the bulk of eukaryotic genomes under unstressed conditions, and are generally regarded as high fidelity [24]. Current models to explain resolution of stalled replication forks invoke specialized polymerases to perform DNA synthesis either at the fork, when replicative polymerases are inhibited [12], or post-replicative gap-filling synthesis behind the replication fork [25]. Specialized polymerases eta (Pol η) and kappa (Pol κ) maintain the integrity of genome duplication through DNA lesions, non-B DNA structures, and common fragile sites (CFS) [12, 26–30]. Correspondingly, replication stress caused by hydroxyurea, aphidicolin, and chemotherapeutic agents induce the up-regulation of Pol η, allowing cells to complete genome replication [31–33]. Recent research has shed some light on the DNA polymerases required to mitigate oncogenic stress. DNA Pol δ facilitates break-induced replication fork repair and cell cycle progression in cells overexpressing Cyclin E [34]. In normal human fibroblasts and cancer cells, Pol κ is important for the tolerance of Cyclin E/CDK2-induced DNA replication stress [35], while Pol η confers tolerance to Myc-induced replication stress in cancer cells [36].

Given their vital roles in maintaining genome stability, we sought to understand the regulation of DNA polymerases in response to oncogene activation, and we focused on cellular responses to mutant *H-RAS*. We discovered that several DNA polymerases are actively depleted in a temporal manner in response to Ras^{G12V} overexpression in human cells. Replicative polymerases appear to be regulated primarily at the transcriptional level, while specialized polymerases are regulated primarily at the post-transcriptional level. Finally, we show that, in SV-40 transformed cells, DNA polymerase depletion in response to Ras^{G12V} signaling is associated with slowed replication fork progression and enhanced Chk2 checkpoint activation. Our study shows that DNA polymerase expression is impacted by *H-RAS* activation, a fact that may contribute to oncogene-induced replication stress or genome instability.

Materials and methods

A detailed list of Key Resources is provided in S1 Table.

Cell culture and reagents

hTERT-immortalized BJ-5a human fibroblasts (CRL-4001™; ATCC) were cultured according to ATCC guidelines in 4:1 mixture of Dulbecco's medium and Medium 1999 supplemented with 10% Hyclone™ FBS (GE Healthcare) and 50 μg/ml Gentimicin (Life Technologies). Experiments were performed between population doublings 10–35. SV40 transformed XPV and *POLH*-complemented cell lines (XP30RO) were a gift from Jean-Sebastian Hoffman (Cancer Research Center, Toulouse, France) and were cultured in Dulbecco's medium, 10% FBS, and 50 μg/ml Gentimicin. Normal diploid IMR90 human fibroblasts (ATCC CCL-186) were cultured according to ATCC guidelines in low oxygen (2% O_2) in DMEM with 10% FBS supplemented with L-glutamine, non-essential amino acids, sodium pyruvate, and sodium bicarbonate. Experiments with IMR90 were performed between population doublings 25–35. Cell lines were confirmed to be free of mycoplasma infection using MycoAlert™ Mycoplasma Detection Kit (Lonza).

Retro and lentiviral packaging and infection

Retrovirus production from pBabe vectors was performed using 293FT phoenix cells and human cell transduction was performed using the BBS/calcium chloride method (15). Lentivirus was packaged using the ViraPowerKit (Thermofisher) following the manufacturer's instructions with modifications. Briefly, pLKO.1 Lentiviral constructs (Addgene) were transfected into 293FT cells using 35 μg polyethylenimine per transfection (Alfa Aesar). After 48 hours of incubation, virus-containing media was collected. The experimental timeline of human cell infections and selection is outlined in Fig 1A. Cells were infected with viruses containing pBabe vector-only (control) or pBabe encoding $HRas^{G12V}$, followed by a second round of infection 24 hours later. 24 hours after the second infection, the cells were replated, and selected with puromycin 6 hours after seeding (2 μg/μl for *hTERT* BJ5a; 1 μg/μl SV40 cell lines). For dual Ras^{G12V} and shRNA lentiviral infections, BJ5a cells were first infected with viruses containing pBabe vector-only or $HRas^{G12V}$ vectors. After 24 hours, a second round of infections was performed simultaneously with viruses containing both pBabe vectors and pLKO.1 vectors as described above. Cells were replated and selected with 4 μg/ml puromycin for 2 days, followed by reseeding for subculture and assays. For infections with inhibitor treatments, infected cells were plated into 10 cm^2 plates the day before the indicated timepoints. After 24 hours, cells were treated with proteasome inhibitor MG132 (Sigma) for 4 hours, followed by protein isolation (described below).

Gene expression analysis

Experiments were performed according to MIQE guidelines with at least three technical replicates for all cell lines and three biological replicates for BJ5a cells. Total RNA was extracted using RNAeasy Kit (Qiagen), assessed for quality using the 2200 TapeStation (Agilent), and 600 ng-1 ug of samples with RIN>9 were converted to cDNA using qScript cDNA Synthesis Kit (Quanta Bioscences). qPCR was performed according to manufacturer guidelines with 20 ng of cDNA, 1X Taqman target and control probes (Life Technologies), and PerfeCTa® Fast Mix® II, Low Rox (Quanta Biosciences). The reactions were analyzed using Agilent QuantStudio 7 Flex.

Immunoblot analysis and quantification

Whole cell extracts were collected by lysing cells with RIPA buffer (Santa Cruz Biotechnology) supplemented with Halt protease and phosphatase inhibitors (Life Technologies) and PMSF

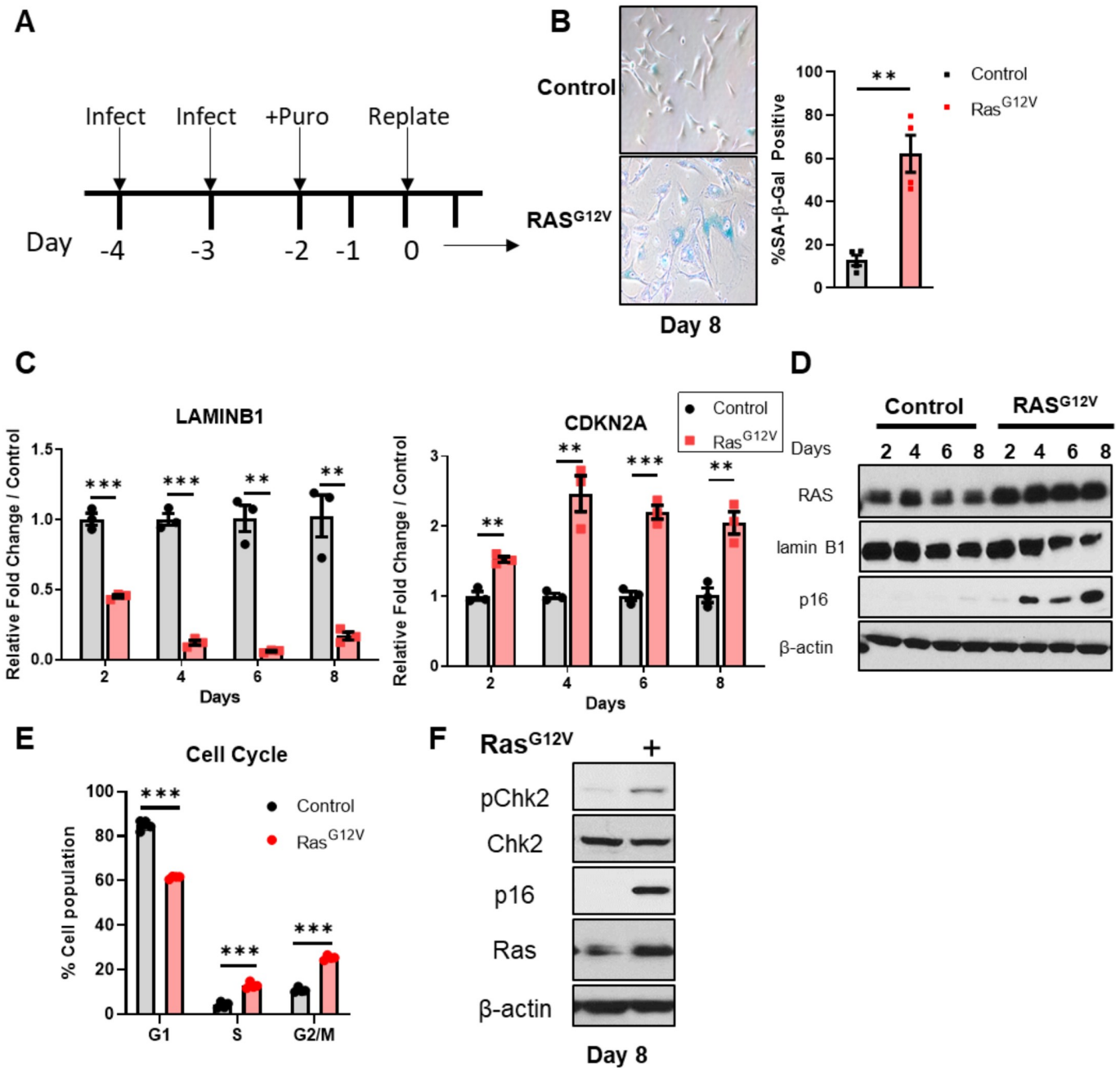

Fig 1. Ras^{G12V} overexpression in h*TERT*-BJ5a cells induces a senescent phenotype. (A) Schematic of the experimental infection and selection time course. (B) *hTERT* BJ5a human fibroblasts were infected with pBabe retrovirus empty vector (control) or encoding mutant Ras^{G12V}. *Left panel*: SA- β-galactosidase staining of BJ5a cells (Day 8) with and without Ras^{G12V} OE. *Right panel*: Quantification of β-galactosidase staining (N = 3 technical replicates). Data represent mean +/- SEM. (C) mRNA expression of senescence markers *LMNB1* and *CDKN2A* after Ras^{G12V} OE. qRT-PCR was performed at the indicated timepoints following selection. Data represent mean +/- SEM of three biological replicates. (D) Corresponding immunoblot analysis of senescence markers LaminB1 and p16. One of three biological replicates is shown. (E) Cell cycle analyses of control and Ras^{G12V} OE cells on Day 8. Data represent mean +/- SD of three biological replicates. (F) Checkpoint activation after Ras OE. Immunoblot analyses for Chk2 Thr38 phosphorylation was performed on Day 8. One of three biological replicates is shown.

https://doi.org/10.1371/journal.pone.0251188.g001

(Santa Cruz). Extracts concentrations were determined using DC™ Protein Assay (Bio-Rad). Sample preps were prepared using 4X LDS Sample buffer and 10X Reducing Agent (Life Technologies) and incubated at 70˚C for 10 min. Samples were loaded into pre-casted NuPage gels (Life Technologies). Gels were electrophoresed in 1X MOPS buffer, transferred onto 0.2um Amersham™ Hybond™ PVDF membranes (GE Healthcare). After transfer, efficiency was visualized by Ponceau S staining and blocked with 5% non-fat milk or BSA in TBS containing 0.1% Tween (TBST) before incubating with primary antibody overnight. Membranes were washed 5 times with TBST for at least 10min and were incubated with mouse or rabbit secondary antibodies at 1:20,000 dilution for 1 hour at room temperature. After washing with TBST for 5 times, blots were visualized with chemiluminescence reagents Amersham™ ECL™ Prime Western Blotting Detection Reagents (GE Healthcare) or Pierce™ ECL Western blotting substrate (Thermofisher). Bands were quantified using ImageJ (NIH) [37]. Briefly, relative intensity was calculated for individual bands per blot. Adjusted intensities were calculated by normalizing relative intensity of each band to its respective β-actin control.

Beta-galactosidase staining

Senescence-associated (SA)-β-galactosidase staining was performed as previously described [38]. Briefly, cells were fixed with 2% formaldehyde/0.2% glutaraldehyde in PBS for 10 min. After washing with PBS, cells were stained at 37˚C in a non-CO_2 incubator with the staining solution (40 mM Na_2HPO_4 pH 5.7, 150 mM NaCl, 2 mM $MgCl_2$, 5 mM $K_3Fe(CN)_6$, 5 mM $K_4Fe(CN)_6$, 1 mg/ml X-gal). After 16 hours, wells were washed with RO water and images were acquired using an inverted microscope (Nikon Eclipse Ti) with a 20X/0.45 objective and a camera (Nikon DS-Fi3).

Immunofluorescence for EdU incorporation

Cells were plated on 22x22 mm glass coverslips the day before indicated time point (Fisher Scientific). Cells were pulsed with 20 μM EdU(5-ethynyl-2'deoxyuridine Lumiprobe) for 1 hour and fixed with 4% paraformaldehyde (Sigma) for 10 min. Cells were washed with PBS and permeabilized with 0.3% Triton-X for 15 min. Reaction mixes were freshly made with 20 uM FAM-azide (Lumiprobe B5130), 4 mM copper sulfate pentahydrate (Sigma), 20 mg/ml ascorbic acid (Sigma) in PBS. Coverslips were labeled with 40 μl reaction mix for 30 min at room temperature. Coverslips were washed twice with PBS and mounted with antifade mounting medium VECTASHIELD with DAPI (Vectorlabs). Images were acquired at room temperature using Zeiss AXIO Microscope Imager.M2 and Apotome.2 apparatus with a 64X oil objective and the Zen Pro software. Representative pictures were obtained using Z-stacks and maximum intensity projections.

Cell cycle analysis

After infection, cells were fixed in 70% ethanol, washed, resuspended with 1% BSA in PBS, and placed in -20˚C for at least overnight until further processing. For standard cell cycle analysis, cells were resuspended with 0.1% Triton-X, 200 μg/ml RNAase, and 40μg/ml propidium iodide. For EdU cell cycle analysis, cells were pulsed with 20 μM EdU for 1 hour. Cells were harvested using trypsinization, fixed with 4% paraformaldehyde for 15 min, and permeabilized with 0.1% saponin (47036-50G-F Sigma) and 1% BSA in PBS (Saponin-BSA buffer) for 15 min. Cells were washed Saponin-BSA buffer and incubated with Click reaction buffer containing 20 μM Sulfo-cyanin5 azide (Lumiprobe B3330), 4mM copper sulfate pentahydrate, and 20 mg/ml ascorbic acide in PBS for 30min. Cells were washed with Saponin-BSA buffer twice and incubated with 200 μg/ml RNAse and 40 μg/ml propidium iodide at 37˚C for 15 min. Samples

were analyzed on BD FACSCanto with FlowJo software. Cells with >4C DNA content were excluded from the analyses.

Clonogenic survival

After retroviral infection, cell populations were selected with puromycin for 2 days, followed by seeding at 1000 cells per well (in triplicate) using 6-well plates. Media was replaced every 2–3 days. After 10–14 days, colonies were fixed with 100% methanol for 10 min and stained with crystal violet solution for 15 min. Wells were destained using 10% acetic acid and the intensities of crystal violet staining were quantified using 590 nm absorbance with a spectrophotometer. Raw values were normalized to a control well with no cells. Survival percentages were calculated as the mean normalized staining values from Ras^{G12V}-infected cells divided by the mean normalized staining values from control-infected cells.

Microfluidics-assisted replication track analysis (maRTA)

Fiber combing analyses were performed as previously described [39, 40]. Briefly, the day before the indicated timepoint, cells were plated in 60 cm plates at 60% confluency overnight. Cells were labelled with 50 μM IdU for 30 min, washed 3 times with PBS, and labelled with 250 μM CldU for 30 min. Cells were trypsinized and washed with agarose insert buffer (10 mM Tris7.5, 20 mM NaCl, 50 mM EDTA in water). After spin down, cells were resuspended in agarose insert buffer and mixed 1:1 with 2% low-melting agarose (Bio-Rad). Gel inserts were solidified at 4˚C overnight and were stored in agarose insert buffer until analysis. Microscopy of stretched DNAs was performed on the Zeiss Axiovert microscope with a 40x objective, and images were captured with the Zeiss AxioCam HRm camera. Fluorochromes were Alexa594 for CldU and Alexa488 for IdU. Lengths of tracks were measured manually in raw merged images using Zeiss AxioVision software, as well as automatically, using an open source software FiberQ [41] with concordant results. Percentages of ongoing (IdU-CldU) or terminated (IdU only) forks, and origin firing events were derived from FiberQ outputs. Statistical significance for track lengths was calculated using Kruskal-Wallis tests followed by pairwise Wilcoxon tests to derive p values adjusted for multiple comparisons. For origin firing percentages, statistical significance was determined in one-way ANOVA with post-hoc analysis with Tukey's test to derive p values adjusted for multiple comparisons. Analyses were done in R Version 3.6.3.

Statistics

Unless stated otherwise, graphical representation and statistical analyses were done using GraphPad Prism v8.4.1. Unless stated otherwise in the figure legends, all statistical analyses were performed using unpaired Student's t-test, two-tailed. $^{*}p<0.05$, $^{**}p<0.01$, $^{***}p<0.005$, $^{****}p<0.001$, n.s., not significant.

Results

Overexpression of oncogenic H-Ras^{G12V} induces differential depletion of DNA polymerases in nontumorigenic human cells

We aimed to elucidate DNA polymerase expression in response to oncogene-induced replication stress, using an established experimental model of *H-RAS* ^{G12V} overexpression (hereafter referred to as Ras^{G12V} OE) [1, 42] and *hTERT*-immortalized BJ5a human fibroblasts, which do not undergo the replicative senescence of primary fibroblasts [43, 44]. In response to oncogene activation, these cells activate a senescence program, followed by some cells escaping

senescence 2–3 weeks after oncogene overexpression [45]. We infected *hTERT*-BJ5a with a constitutively active, Ras^{G12V} expressing retroviral vector or an empty vector control, followed by puromycin selection for stable transductants (Fig 1A). As expected, we observed an induction of several senescent phenotypes over the course of several days in Ras^{G12V} OE cells, including increased senescence-associated (SA)-β-galactosidase staining, decreased laminB1 expression and increased CDKN2A/p16 expression, compared to control-infected cells (Fig 1B–1D). After 8 days of Ras^{G12V} OE, we measured significantly altered cell cycle distributions and increased CHK2-Thr38 phosphorylation (Fig 1E and 1F). Together, these data show the expected onset of senescent phenotypes and increased DNA damage checkpoint response after Ras^{G12V} OE.

Next, we measured the expression of several DNA polymerase genes in Ras^{G12V} and control infected cells, as a function of days following oncogene overexpression and the onset of senescent phenotypes. Strikingly, we observed significant downregulation of several replicative polymerase genes, including *POLA1*, *POLD1*, *POLD3*, and *POLE*, after $Ras^{G12\ V}$ OE as early as day 2 post selection, and sustained through day 8 (Fig 2A). In contrast, we found only transient and slight downregulation of specialized polymerase genes *POLH* and *POLK* at Day 4, while the DNA repair polymerase *POLB* gene expression was not affected at any time point measured.

DNA polymerase protein levels were also significantly and differentially impacted by Ras^{G12V} OE (Fig 2B). The catalytic subunit of replicative Pol α was depleted as early as day 2. Moreover, production of Pols η, κ, and both catalytic (p125; *POLD1* gene) and accessory (p68; *POLD3* gene) Pol δ subunits was significantly depleted after 8 days. However, similar to its mRNA expression, Pol β protein levels are not altered after Ras^{G12V} OE. Taken together, these results show that DNA polymerases are differentially regulated at the transcript and protein levels in response to oncogenic Ras^{G12V} overexpression.

Ras^{G12V} induced depletion of DNA polymerases is dependent on the proteasomal degradation pathway

We tested whether the depletion of DNA polymerase proteins after Ras^{G12V} OE is due to proteasomal degradation. For each time point after Ras^{G12V} OE, *hTERT*-BJ5a cells were treated with MG132, a 26S proteasome inhibitor, for 4 hours immediately prior to harvesting cell lysates for analysis. Remarkably, we observed a robust rescue of specialized Pols η and κ at multiple timepoints (Fig 3A and 3B; S1 Fig) in treated cells expressing Ras^{G12V}. Notably, the levels of rescue diminish over time after Ras^{G12V} expression. Pols η and κ protein levels are also slightly increased after MG132 treatment of control cells, consistent with previous reports [46, 47]. In contrast, we observed little to no rescue of Pols α (catalytic subunit) or δ (p125 or p68 subunits) in BJ5a cells (Fig 3A and 3B). This result is consistent with replicative polymerase regulation in response to Ras^{G12V} OE occurring primarily at the transcriptional level (Fig 2A). To examine the generality of this response, we repeated this experiment using IMR90 primary fibroblasts. Pols η, κ, and δ are again depleted after Ras^{G12V} OE, and this degradation can be rescued, at least in part, by MG132 treatment (Fig 3C). Together, these data are consistent with DNA Pols η and κ levels being primarily regulated post-transcriptionally and, in part, through the proteasome degradation pathway, under Ras^{G12V} signaling.

Correlation of senescence-associated $p16^{INK4A}$ and DNA polymerase depletion in response to Ras^{G12V} overexpression

The tumor suppressor gene *CDKN2A* ($p16^{INK4A}$) is a major regulator of senescence [48–50]. To ascertain whether $p16^{INK4A}$ plays a role in the observed DNA polymerase depletion, we

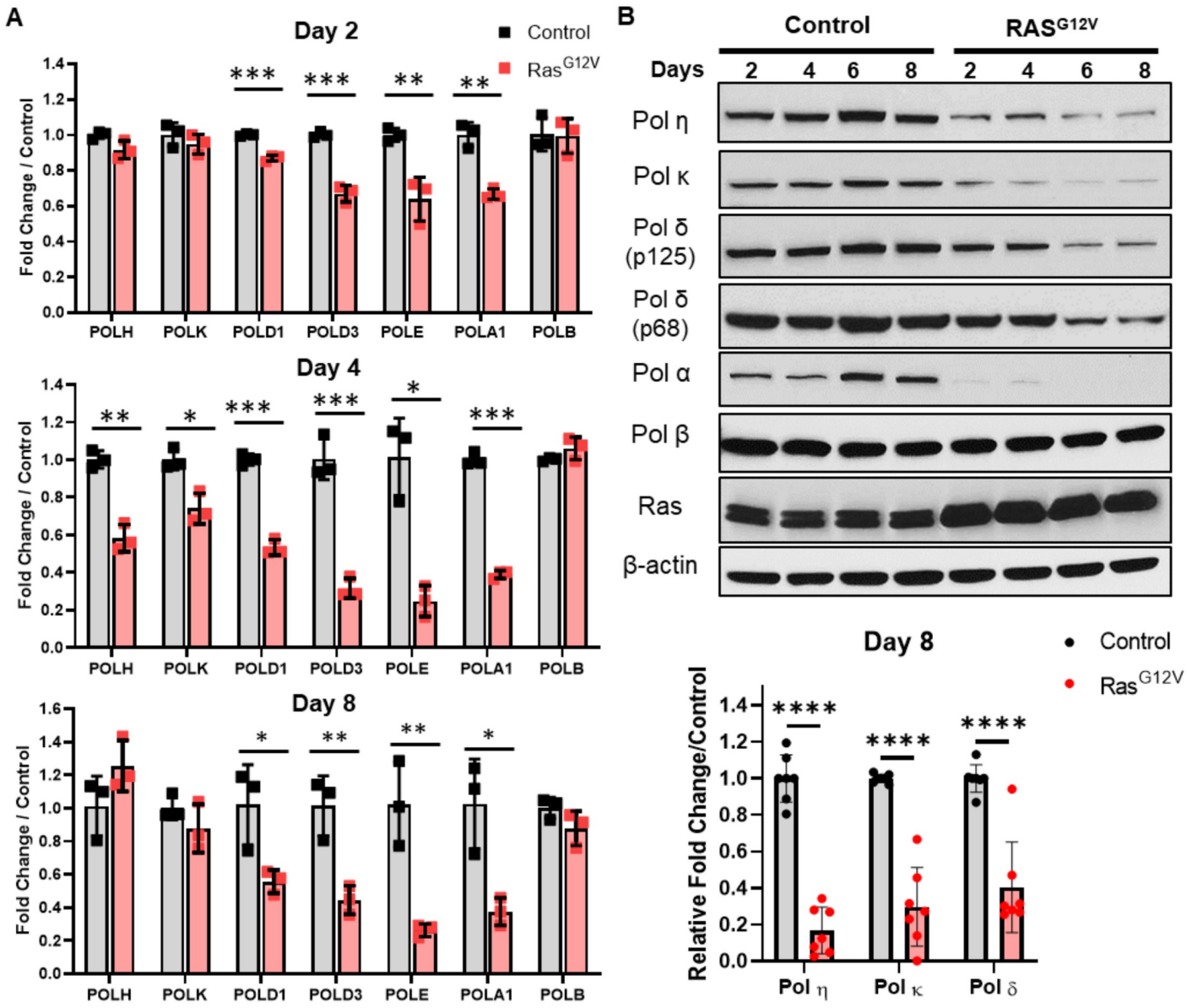

Fig 2. Overexpression of oncogenic Ras^{G12V} induces downregulation of replication fork-associated DNA polymerases. (A). *hTERT* BJ5a human fibroblasts were infected with pBabe retrovirus empty vector (control; gray bars) or encoding mutant Ras^{G12V} (red bars). POL gene expression was determined using qRT-PCR at the indicated timepoints after selection. Data represent mean +/- SEM of three biological replicates. (B). *Top panel*-Immunoblot analyses of representative control and Ras^{G12V} -infected cell populations at indicated timepoints. One of three biological replicates is shown. *Bottom panel*- Quantification of DNA polymerase protein levels 8 days after control or Ras^{G12V} transduction. Data represent mean +/- SD of seven biological replicates.

https://doi.org/10.1371/journal.pone.0251188.g002

used an shRNA approach to knockdown *CDKN2A* (p16 ^{INK4A}) expression after Ras^{G12V} infection (Fig 4A). At the transcript level, we observed no significant change in the expression of the polymerase genes examined after *CDKN2A* knockdown (Fig 4B). At the protein level, p16^{INK4A} levels were the lowest in Ras^{G12V} OE + sh*CDKN2A* cells at day 2. After 8 days of Ras^{G12V} OE, p16 levels are elevated even in the presence of lentiviral sh*CDKN2A* (Fig 4C). While we observed some increase in Pols α, δ (p125), and κ levels with p16 knockdown, these effects were variable and not statistically significant (Fig 4D). However, we did observe a pattern that Pol η protein expression may be inversely correlated with the presence of p16^{INK4A}.

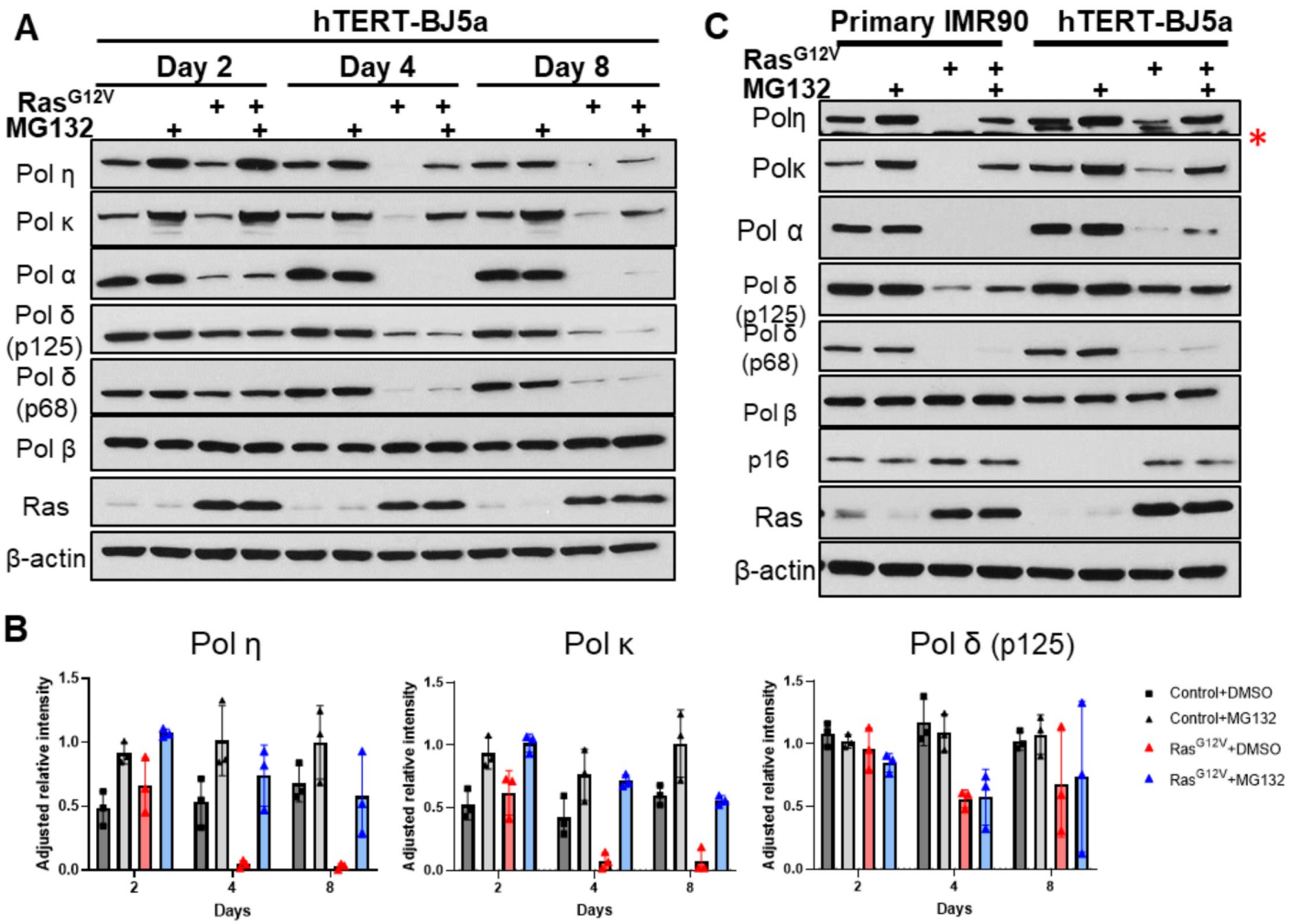

Fig 3. DNA polymerases η and κ levels are regulated by the proteasome degradation pathway. (A) Immunoblot analyses of polymerase levels at indicated days after transduction and selection with control or Ras^{G12V} vectors. *h-TERT* BJ5a cells were either treated with DMSO or MG132 (10μM) for 4 hours prior to harvesting. Immunoblot analysis represent one of three biological replicates (see S1 Fig for additional replicates). (B) Relative polymerase levels in BJ5a cells. Adjusted relative intensity values were calculated using ImageJ; data are from three biological replicates. (C) Side-by-side comparison of primary fibroblast IMR90 and BJ5a cells infected with control or Ras^{G12V} at day 8. Cells were treated with DMSO or MG132 (10 μM) for 4 hours prior to harvest. The BJ5a results shown here are an independent biological replicate of Fig 3A. *Asterisk indicates a non-specific band.

https://doi.org/10.1371/journal.pone.0251188.g003

Pol η depletion is sufficient to induce a senescence-like growth arrest

Both Pol η and Pol κ play important roles in genome duplication, DNA damage, and the replication stress response [11, 12, 29]. We and others have shown that Pol η mRNA and protein levels are increased in tumor cells in response to exogenous sources of replication stress [31–33]. Therefore, the $HRas^{G12V}$-induced depletion of Pols η and κ in cells undergoing senescence was surprising. However, previous reports have hinted that Pol η may play a role in regulating senescence. Pol η knockout mice display metabolic abnormalities and increased senescence-associated phenotypes specifically in adipocytes [51]. Pol η also could suppress senescence because it participates in the alternative lengthening of telomeres (ALT) pathway [52]. Therefore, we tested directly whether loss of Pol η expression is sufficient to induce senescence. To do so, we transduced *hTERT*-BJ5a cells with lentiviral *POLH* shRNAs. Strikingly, we found a

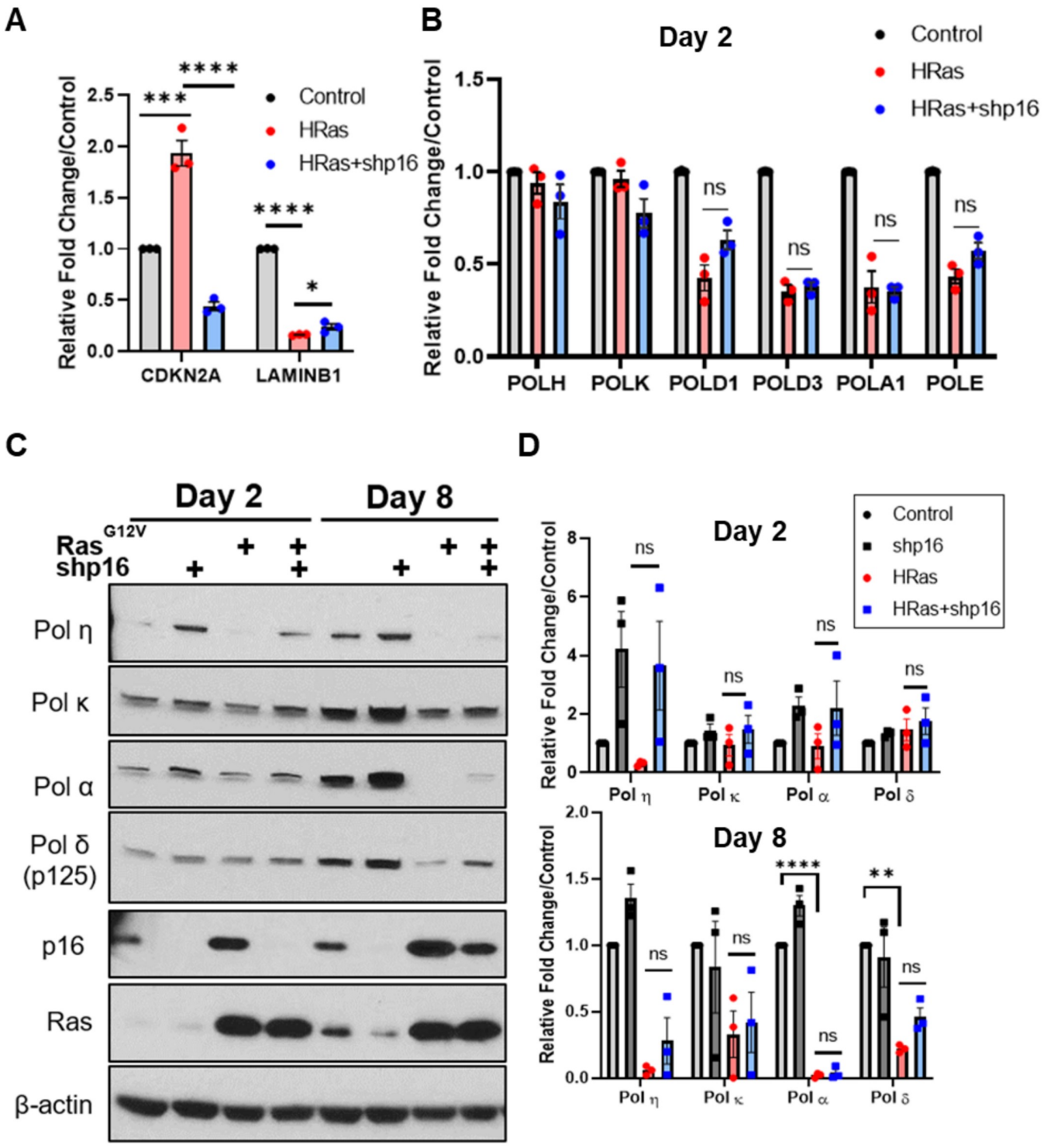

Fig 4. Relationship of p16 to DNA polymerase expression in response to oncogenic Ras^{G12V} signaling. *hTERT*-BJ5a cells were infected with lentivirus expressing short hairpin RNAs (shRNAs) targeting *CDKN2A*. Scrambled shRNA was used as control. (A) mRNA expression analysis of senescence markers on Day 2 as determined using qRT-PCR. (B) mRNA analyses of DNA polymerase gene expression on Day 2 as determined using qRT-PCR. Data represent mean +/- SEM from three biological replicates. Statistical analyses were performed using One-way ANOVA with Tukey's post-hoc. n.s., not significant. $^{*}p<0.05$, $^{***}p<0.005$, $^{****}p<0.0001$. (C) Immunoblot analyses of control or Ras^{G12V} BJ5a cells, with and without p16 knockdown. Data are representative of three independent replicates. (D) Quantification of control or Ras^{G12V} BJ5a cells immunoblot analyses, with and without p16 knockdown. Statistical analyses were performed using One-way ANOVA with Tukey's post-hoc. $^{**}p<0.005$, $^{****}p<0.0001$, n.s., not significant.

https://doi.org/10.1371/journal.pone.0251188.g004

significant reduction of Pol α protein expression (Fig 5A and 5B) concomitant with *POLH* knockdown. *POLH* knockdown cells also exhibited increased p16 expression, compared to controls (Fig 5C). *POLH* depletion reduced the number of EdU positive cells on both days 2 and 8 (Fig 5D). *POLH* knockdown also increased SA-β-galactosidase staining and decreased clonogenic survival (Fig 5E and 5F). Taken together, these results suggest that depletion of Pol η is associated with decreased Pol α and increased p16 expression and is sufficient to induce a senescence-like growth arrest.

DNA polymerase degradation in response to Ras^{G12V} in SV40 transformed cells is associated with altered replication fork dynamics

DNA polymerase levels can be altered in human tumors (8); specifically, *POLH* is upregulated or amplified in melanoma, esophageal and ovarian cancer [28, 32, 53, 54], which contrasts with the $HRas^{G12V}$-induced depletion we measured above in nontumorigenic cells. Therefore, we next asked whether the degradation of DNA polymerases after oncogene activation persists in transformed cells. To mimic a tumor-like model, we used immortalized, SV40 virus-transformed XPV30RO fibroblasts (SXPV) [55], in which the p53, Rb, and other cancer-associated signaling pathways are disrupted. To mimic the increased expression of Pol η observed in tumors, we utilized genetically related SV40 transformed, *POLH*-complemented XPV30RO cells (SXPVη), which overexpress Pol η [56]. Similar to our observation using *hTERT* and primary cell lines, Ras^{G12V} OE in SXPVη cells led to a rapid depletion of Pols α, η, κ and δ (p68 subunit) as early as day 2 and sustained through Day 8; however, depletion of the Pol δ catalytic p125 subunit was not observed (Fig 6A). Moreover, the depletion of exogenous Pol η in SXPVη (*POLH*-complemented) cells is further evidence that the regulation of Pol η is post-transcriptional.

In striking contrast, we observed no depletion of any DNA polymerase analyzed in genetically related SXPV (Pol η-deficient) cells after Ras^{G12V} OE (Fig 6A). Having this pair of cell lines with distinct responses afforded us the opportunity to investigate the consequences of Ras-induced polymerase degradation on cellular processes. Replicative Pols α and δ are required for the bulk of on-going genome replication [10]. Therefore, we asked what impact the depletion of Pol α DNA polymerase catalytic subunit (p180) and Pol δ accessory subunit (p68) has on cell cycle progression and DNA replication. In both SXPV and SXPVη cells, Ras^{G12V} OE resulted in similar cell cycle changes (Fig 6B), relative to the corresponding control infected cells, with increased populations of cells in G1and G2 phases and decreased populations of cells in S phase (Fig 6C). However, even after 8 days of Ras^{G12V} OE, both SXPV and SXPVη populations retain ~30–40% of EdU+, S phase cells, despite the differential DNA polymerase expression. Typically, cells undergoing replication stress display slower fork progression, which can be compensated by increased origin firing [2]. Using DNA fiber analyses, we determined that the depletion of DNA polymerases in SXPVη cells after Ras^{G12V} OE led to a significant decrease in the length of ongoing and terminated forks, as expected for fork slowing (Fig 6D and 6E). However, we measured no increase in origin firing (Fig 6F), possibly due to low Pol α levels, a critical enzyme required for origin activation. In contrast, in Ras^{G12V}-infected SXPV cells where DNA polymerases α and others are present, we observed no changes in fork progression (Fig 6D and 6E). Instead, Ras^{G12V}-infected SXPV cells displayed increased origin firing, compared to control infected cells (Fig 6F). Together, these data suggest that depletion of DNA polymerases in SXPVη cells after 8 days of Ras^{G12V} leads to reduced replication fork elongation but no significant changes in origin activation.

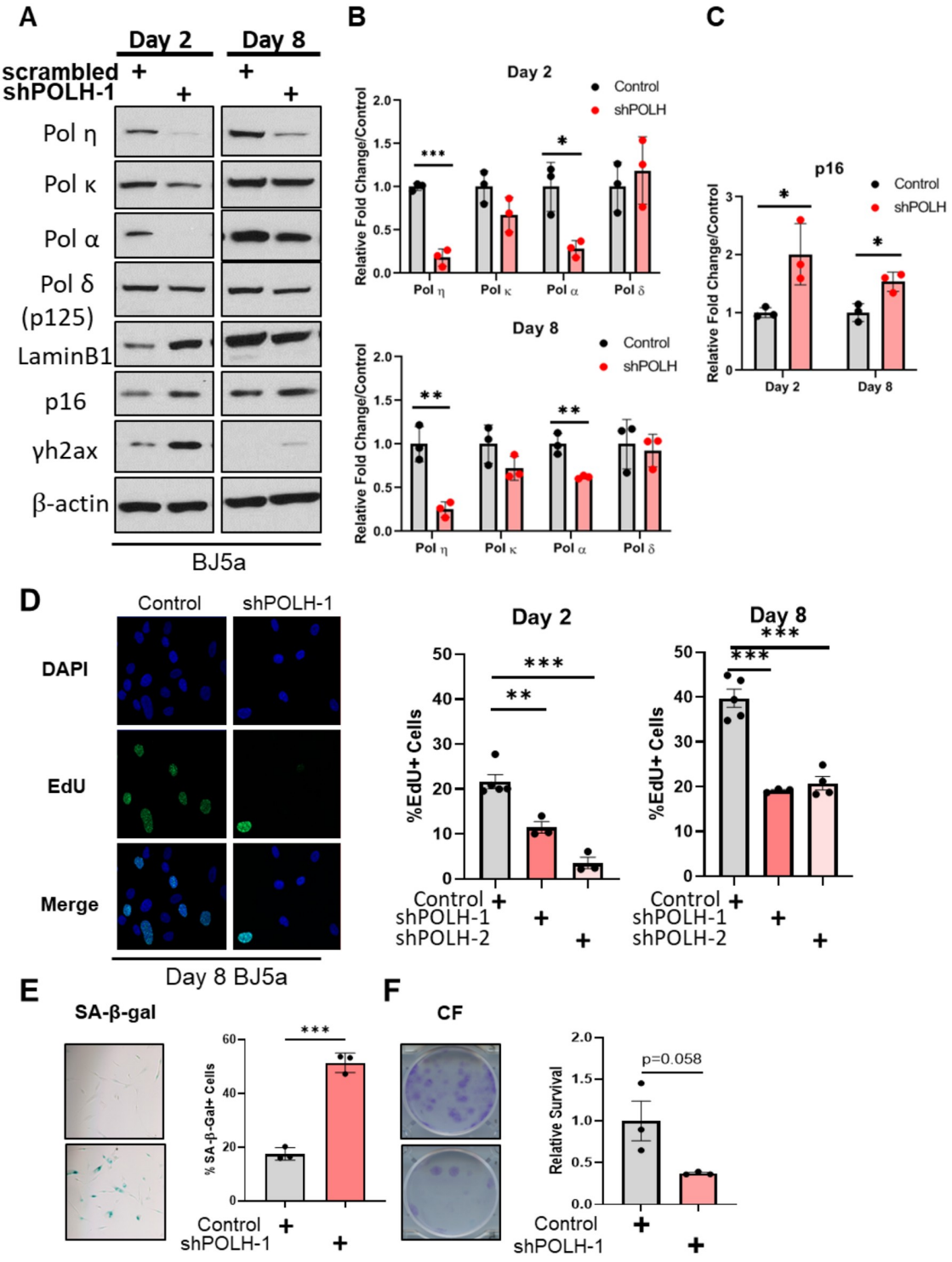

Fig 5. DNA polymerase η depletion is sufficient to induce a senescence-like growth arrest. (A). *hTERT*-BJ5a cells were infected with lentivirus expressing shRNA targeting *POLH*. Scrambled shRNA was used as control. Immunoblot analyses of indicated proteins at days 2 and 8 after lentivirus infection is representative of three biological replicates. (B). Quantification of immunoblot analyses of BJ5a cells infected with *POLH* or scrambled shRNA lentivirus at days 2 and 8. Data represent mean +/- SD of three biological replicates. (C). Quantification of p16 expression in BJ5a cells infected with *POLH* or scrambled shRNA lentivirus at days 2 and 8. Data represent mean +/- SD of three biological replicates. (D). Quantification of EdU positive cells (by immunofluorescence) of either two separate shRNA clones or scrambled shRNA at indicated days. Data represent mean +/- SEM for at least three biological replicates with two technical replicates. (E). Quantification of SA-β-gal activity at Day 8. Data represent mean +/- SEM for

three biological replicates. (F). Quantification of clonogenic survival (crystal violet staining intensity) at Day 14. Data represent mean +/- SEM for three biological replicates.

https://doi.org/10.1371/journal.pone.0251188.g005

DNA polymerase degradation in response to Ras^{G12V} in SV40 transformed cells is associated with checkpoint induction

Oncogene-induced replication stress is well known to increase markers of DNA damage; therefore, we examined activation of the DNA damage response in both cell lines. In SXPVη cells (with polymerase degradation), we observed a very robust increase in Thr68 phospho-Chk2 after 8 days of Ras^{G12V} OE, accompanied by a dramatic depletion of total Chk1 protein expression (Fig 7A). This observation is consistent with previous findings that cells suppress and deplete total Chk1 protein during genotoxic stress and nutrient deprivation via the senescence or the autophagy program [57–60], perhaps as a mechanism of terminating the S phase checkpoint [61]. In contrast, after 8 days of Ras^{G12V} OE, SXPV cells (without polymerase degradation) showed less robust activation of Thr68 phospho-Chk2, while Chk1 was constitutively phosphorylated (Ser 345) (Fig 7A). Thus, polymerase depletion in response to Ras^{G12V} OE is correlated not only with altered fork progression, but also with differential checkpoint activation. Finally, we examined the ability of cells to survive prolonged oncogene overexpression. After 10 days of Ras^{G12V} OE, we measured a significantly greater survival of SXPVη cells, relative to control infected cells, as compared to SXPV cells (Fig 7B and 7C). Thus, the presence of Pol η appears to improve the ability of cells to survive Ras^{G12V} OE. Perhaps, DNA polymerase depletion in response to Ras^{G12V} signaling allows cells to adapt to oncogene-induced replication stress by limiting replication fork progression and enforcing checkpoint activation, which ultimately improves cell survival.

Discussion

DNA replication is a crucial phase of mitotic cell growth, as it represents the time during which the genome is most vulnerable to damage and mutation. DNA polymerases are integral to all replication process, including ongoing fork elongation, fork restart, and fork repair. Despite their central role in replication, much remains unclear about the regulation of DNA polymerases in response to oncogene-activation. In this study, we investigated the consequences of mutant H-Ras^{G12V} overexpression on DNA polymerase expression levels in human cells, focusing on a subset of polymerases known to be engaged at the replication fork. To our knowledge, our study is the first to report the robust cellular response to oncogenic Ras activation that depletes multiple DNA polymerases. Our results suggest that distinct mechanisms regulate replicative *versus* specialized DNA polymerases in response to Ras^{G12V} overexpression: replicative polymerases are primarily regulated at the gene level (Figs 2 and 4), while specialized polymerases are primarily regulated at the protein level (Figs 2 and 3). Taken together, our study has uncovered a novel cellular response to oncogene activation that is distinct from the response to replication stress induced by DNA damaging agents or drugs, from the perspective of DNA polymerase regulation. This discovery has important implications for how human cells regulate DNA polymerases to limit DNA synthesis in response to endogenous replication stress.

Oncogenic Ras^{G12V} overexpression in nontumorigenic cells induces an initial hyperproliferative response, followed by cellular senescence [1, 2, 62]. This response is accompanied by markers of replication stress, such as decreased fork elongation rate and increased DNA damage. Many mechanisms have been identified that contribute to oncogene-induced replication

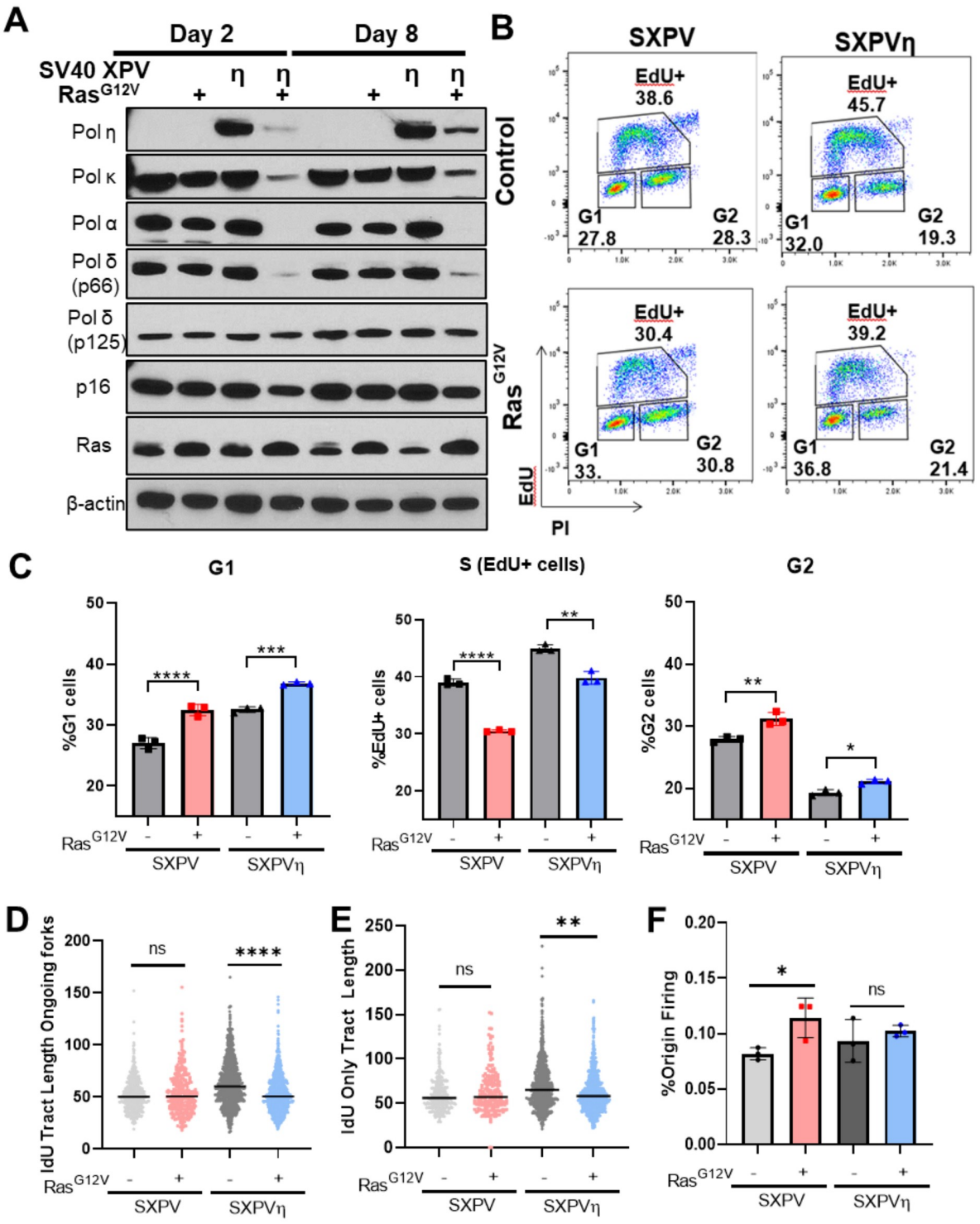

Fig 6. Differential oncogenic Ras^{G12V}-induced DNA polymerase depletion is associated with altered replication fork dynamics. (A). Immunoblot analysis of SV40-transformed XPV cells (SXPV) and *POLH*-complemented SV40-transformed XPV cells (SXPVη), infected with control or Ras^{G12V} at Days 2 and 8. One of four biological replicates is shown. (B). Representative cell cycle analyses of SXPV/SXPVη cell populations infected with control vector or Ras^{G12V} at Day 8. (C). Quantification of cell populations (B) from three biological replicates. (D). DNA fiber combing assay for ongoing (IdU-CldU) forks. Data represent IdU lengths of IdU-CldU tracts from two biological replicates. Statistical analysis was performed using Wilcoxon rank sum test with Holm's post-hoc test. $^{****}p<0.0001$. n.s., not significant. (E). DNA fiber combing assay for terminated (IdU only) forks. Data represent IdU tract lengths from IdU only fiber of two biological replicates. Statistical analysis was performed using Wilcoxon rank sum test with Holm's post-hoc test. $^{**}p<0.01$. n.s., not significant. (F). DNA fiber

combing assay for origin firing. Percent origin firing was calculated using CldU only and CldU-IdU-CldU tracts / total tracts. Origin firing data is from three biological replicates.

https://doi.org/10.1371/journal.pone.0251188.g006

stress, including dysregulated replication initiation, altered nucleotide metabolism, transcriptional R-loops, and oxidative stress [1, 2, 5, 15, 63]. Here, we demonstrate a dramatic downregulation/degradation of DNA polymerases that are required for ongoing fork elongation, which we propose might contribute directly to oncogene-induced replication stress. Using SV40 transformed cell lines, we observed that cells undergoing oncogene-induced polymerase degradation display the decreased replication fork progression characteristic of replication stress, whereas fork lengths do not change in XPV30R0 cells without DNA polymerase degradation (Fig 6). After 8 days of Ras^{G12V} OE, we observed that cell populations with reduced replicative polymerase levels retain EdU^+, S-phase cells, albeit with slowed replication forks (Fig 6). Our observation that levels of the Pol α catalytic subunit were low to undetectable in SV40 Ras^{G12V} OE cells, despite retaining EdU^+ cells, was unexpected and warrants further investigation. One possible explanation of our results is that Pol α formation of initiator DNA from RNA primers created by the Pol α primase subunits is not an absolute requirement for ongoing lagging strand synthesis, and that the Pol δ holoenzyme can extend RNA primers directly. This hypothesis is based on a recent *in vitro* study of eukaryotic replisomes [64]. Using single molecule analyses and purified *S. cerevisiae* replication proteins, Lewis *et al.* propose that Pol α DNA synthesis activity is not absolutely required during processive leading/lagging strand replications; rather, only the primase activity of Pol α-primase is required [64]. We did not examine levels of the primase subunits of the Pol α holoenzyme before and after Ras^{G12V} OE. An alternative (not mutually exclusive) hypothesis to explain our results is that PrimPol is activated in response to Ras^{G12V} OE to compensate for the lost functions of DNA Pol α during ongoing fork elongation. We did not examine PrimPol levels in our study; however, under stress condition, the PrimPol enzyme is known to assist in DNA replication [65–68]. Lastly,

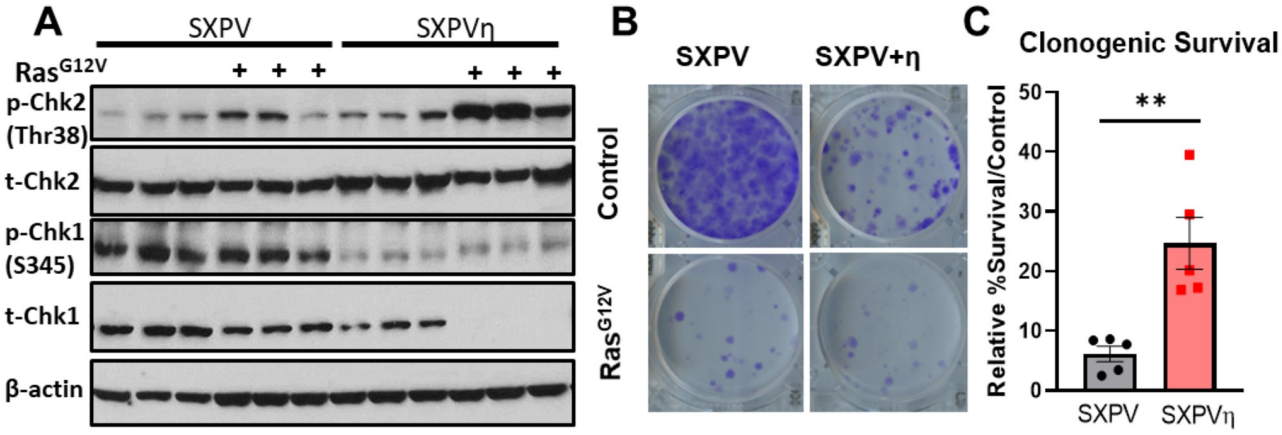

Fig 7. Oncogenic Ras^{G12V}-induced DNA polymerase depletion is associated with altered checkpoint signaling. (A). Immunoblot analysis of control or Ras^{G12V}-infected SXPV/SXPVη cells for indicated checkpoint proteins. All three biological replicates are shown. (B). Representative crystal violet staining of control-infected or Ras^{G12V}-infected SXPV/SXPVη cells at Day 10. Each cell line was selected with puromycin for 2 days after retroviral infection, followed by seeding at 1000 cells per well (in triplicate). Media was replaced every 2–3 days. After 10 days, colonies were fixed with methanol and stained with crystal violet. (C). Quantitation of survival in Ras^{G12V}-infected SXPV/SXPVη cells at Day 10, relative to respective controls. The intensity of crystal violet staining in each well was quantified using 590 nm absorbance after destaining. Raw values/well were normalized to a control well with no cells. Survival percentages were calculated as the ratio of normalized mean values from Ras^{G12V}-infected wells to mean values from control-infected wells. Data represent mean +/- SEM of five biological replicates.

https://doi.org/10.1371/journal.pone.0251188.g007

we measured robust Chk2 activation concomitant with Chk1 depletion in cells undergoing oncogene-induced polymerase degradation (Fig 6). Pol α and Pol κ both mediate *ATR* activation via the 9-1-1 complex [69, 70], and we show that both polymerases are targets for Ras-induced depletion. Perhaps, the depletion of polymerases associated with the replication fork and required for *ATR* activation contributes to cell cycle checkpoint enforcement.

An *H-RAS*-induced senescence-associated protein degradation (SAPD) response has been reported, in which proteins are selectively degraded in an *ERK* and proteasome dependent process [71]. Consistent with this report, we demonstrate that proteasome inhibition partially rescued polymerase proteins, suggesting that SAPD may be responsible, in part, for Ras^{G12V}-induced polymerase depletion. Pol η is heavily targeted for depletion and re-localization after DNA damage through several post-translational modifications, including phosphorylation, ubiquitination and SUMOylation [46, 72–75]. Pol η also can be regulated indirectly via Rad18 phosphorylation through *JNK* signaling, another major pathway downstream of RAS [72]. The *RAS* family of proto-oncogenes (K-, H, N-Ras) mediate vital cellular processes such as growth, survival, metabolism, through several mitogenic pathways [17]. More experiments are required to unravel the complex signaling pathways underlying DNA polymerase regulation downstream of the *RAS* signaling axes and advance our understanding of the cellular replication stress response to oncogene activation.

Previous studies have provided indirect evidence that Pol η or κ depletion may result in senescence phenotypes [51, 52, 76]. Here, we report that *POLH* knockdown in *hTERT* BJ5a cells directly induces a senescent-like phenotype (Fig 5). Pol η depletion also significantly reduced Pol α expression, but unlike Ras OE, levels of other polymerases such as Pols κ and δ were not altered. These results suggest that DNA polymerase depletion may be dependent on the mechanisms inducing senescence. One conceivable mechanism that should be explored further is that the cellular depletion of Pol η induces senescence by increasing replication stress [31].

The coordinated degradation of replicative polymerases has been observed in fission yeast as a response to replication stress induced genetically in ΔSwi1 cells (ortholog of timeless) [77]. In that study, the forced accumulation of replication proteins was accompanied by excessive mitotic aberrations, suggesting that the degradation of replisome components plays a critical role in maintaining genome stability. We observed that Ras^{G12V} overexpression significantly downregulated the Pol α catalytic subunit and the Pol δ catalytic subunit. Extensive genetic studies using an *S. cerevisiae* model demonstrated that reduced expression of either Pol α or Pol δ induces substantially elevated rates of chromosomal loss and instability [78]. Extrapolating from this yeast model to our study here, one could surmise that a temporal window of increased susceptibility to genome instability exists after oncogene activation. The Pol δ accessory subunit, p68 (*POLD3*) has a major effect on Pol δ's PCNA binding affinity [79] and mediates Pol δ's retention in the replisome [64]. Our discovery that p68 also is a target for Ras-induced degradation is provocative, given that p68 (*POLD*3) is required for break-induced replication [34, 80] and for mitosis-associated DNA synthesis [81].

Our discovery of Ras^{G12V}-induced DNA polymerase depletion has significant implications for understanding genome instability during carcinogenesis. Overexpression of oncogenes such as Ras^{G12V} and Cyclin E induce a unique landscape of CFS breakage [19]. Fragile sites may contain difficult to replicate sequences (DiToRS), such as microsatellite sequences, non-B DNA structures, and R-loops, that are prone to double strand breaks (reviewed in [28, 63]. Specialized polymerases Pols η and κ are able to efficiently replicate DiToRS [30, 82], and Pol η-deficient cells display elevated levels of replication stress and CFS breakage [27, 31, 83]. Our findings here of Ras-induced Pol η and κ depletion raise the possibility that altered polymerase levels in cells undergoing oncogene activation contribute to genome instability such as the

expression of CFS during neoplastic progression. Moreover, it remains unclear how depletion or altered regulation of DNA polymerases during oncogene activation impacts DNA replication and repair mechanisms. One intriguing question is whether different oncogenes have differential impacts on polymerase expression levels, and whether this regulation is based on oncogene-induced replication stress intermediates, such as depleted nucleotides or unusual DNA secondary structures. For example, hydroxyurea induces replication stress by depleting nucleotide pools and requires Pol κ for replication stress tolerance [76]. Recent studies have shown that Pol κ is preferentially utilized in Cyclin E/CDK2-mediated oncogenic stress [35], and the level of nuclear Pol κ is increased after treatment with *BRAF*, *MEK*, or *ERK* inhibitors [84]. In contrast, another replication stress inducer, aphidicolin, stalls DNA replication by inhibiting replicative polymerases and requires Pol η for tolerance (27,31), and Pol η is utilized in Myc-mediated oncogenic stress (36). Together, current evidence supports the supposition that specific DNA polymerases are better suited for alleviating different causes of replication stress. Thus, elucidating the exact replication intermediates and signaling pathways that mediate DNA polymerase regulation, recruitment, and fork progression will be crucial to understanding the mechanisms underlying oncogene-induced replication stress and the roles of DNA polymerases in promoting tumorigenesis.

Supporting information

S1 Table. List of key resources.
(PDF)

S1 Fig. Replicates for Ras-infected BJ5a cells treated with MG132 inhibitor. Immunoblot analyses of polymerase levels at indicated days after transduction/selection with control or Ras^{G12V} vectors. BJ5a cells were either treated with DMSO or MG132 (10μM) for 4 hours prior to harvesting. Red values are quantification of polymerase levels, normalized to Control or Ras^{G12V} treated with DMSO.
(TIF)

S1 File. Original, uncropped images for all immunoblots.
(PDF)

Acknowledgments

We thank Kelly Leon for expert technical assistance, and the Penn State Cancer Institute Flow Cytometry Core Facility. We are grateful to our colleagues for critical reading of our manuscript and useful suggestions for improvement.

Author Contributions

Conceptualization: Wei-chung Tsao, Kristin A. Eckert.

Data curation: Wei-chung Tsao.

Formal analysis: Wei-chung Tsao, Julia M. Sidorova, Kristin A. Eckert.

Funding acquisition: Katherine M. Aird, Julia M. Sidorova, Kristin A. Eckert.

Investigation: Wei-chung Tsao, Julia M. Sidorova.

Methodology: Wei-chung Tsao, Raquel Buj, Katherine M. Aird, Julia M. Sidorova, Kristin A. Eckert.

Project administration: Kristin A. Eckert.

Resources: Raquel Buj, Katherine M. Aird, Julia M. Sidorova, Kristin A. Eckert.

Supervision: Katherine M. Aird, Kristin A. Eckert.

Visualization: Wei-chung Tsao.

Writing – original draft: Wei-chung Tsao.

Writing – review & editing: Wei-chung Tsao, Raquel Buj, Katherine M. Aird, Julia M. Sidorova, Kristin A. Eckert.

References

1. Di Micco R, Fumagalli M, Cicalese A, Piccinin S, Gasparini P, Luise C, et al. Oncogene-induced senescence is a DNA damage response triggered by DNA hyper-replication. Nature. 2006; 444(7119):638–42. https://doi.org/10.1038/nature05327 PMID: 17136094
2. Kotsantis P, Petermann E, Boulton SJ. Mechanisms of Oncogene-Induced Replication Stress: Jigsaw Falling into Place. Cancer Discov. 2018; 8(5):537–55. https://doi.org/10.1158/2159-8290.CD-17-1461 PMID: 29653955
3. Bartkova J, Horejsí Z, Koed K, Krämer A, Tort F, Zieger K, et al. DNA damage response as a candidate anti-cancer barrier in early human tumorigenesis. Nature. 2005; 434(7035):864–70. https://doi.org/10.1038/nature03482 PMID: 15829956
4. Michaloglou C, Vredeveld LC, Soengas MS, Denoyelle C, Kuilman T, van der Horst CM, et al. BRAFE600-associated senescence-like cell cycle arrest of human naevi. Nature. 2005; 436 (7051):720–4. https://doi.org/10.1038/nature03890 PMID: 16079850
5. Zeman MK, Cimprich KA. Causes and consequences of replication stress. Nat Cell Biol. 2014; 16(1):2–9. https://doi.org/10.1038/ncb2897 PMID: 24366029
6. Zhu W, Abbas T, Dutta A. DNA replication and genomic instability. Adv Exp Med Biol. 2005; 570:249–79. https://doi.org/10.1007/1-4020-3764-3_9 PMID: 18727504
7. Gaillard H, García-Muse T, Aguilera A. Replication stress and cancer. Nat Rev Cancer. 2015; 15 (5):276–89. https://doi.org/10.1038/nrc3916 PMID: 25907220
8. Lange SS, Takata K, Wood RD. DNA polymerases and cancer. Nat Rev Cancer. 2011; 11(2):96–110. https://doi.org/10.1038/nrc2998 PMID: 21258395
9. Lee M, Zhang S, Wang X, Chao HH, Zhao H, Darzynkiewicz Z, et al. Two forms of human DNA polymerase delta: Who does what and why? DNA Repair (Amst). 2019; 81:102656.
10. Burgers PMJ, Kunkel TA. Eukaryotic DNA Replication Fork. Annu Rev Biochem. 2017; 86:417–38. https://doi.org/10.1146/annurev-biochem-061516-044709 PMID: 28301743
11. Bournique E, Dall'Osto M, Hoffmann JS, Bergoglio V. Role of specialized DNA polymerases in the limitation of replicative stress and DNA damage transmission. Mutat Res. 2018; 808:62–73. https://doi.org/10.1016/j.mrfmmm.2017.08.002 PMID: 28843435
12. Sale JE, Lehmann AR, Woodgate R. Y-family DNA polymerases and their role in tolerance of cellular DNA damage. Nat Rev Mol Cell Biol. 2012; 13(3):141–52. https://doi.org/10.1038/nrm3289 PMID: 22358330
13. Bartek J, Bartkova J, Lukas J. DNA damage signalling guards against activated oncogenes and tumour progression. Oncogene. 2007; 26(56):7773–9. https://doi.org/10.1038/sj.onc.1210881 PMID: 18066090
14. Liu XL, Ding J, Meng LH. Oncogene-induced senescence: a double edged sword in cancer. Acta Pharmacol Sin. 2018; 39(10):1553–8. https://doi.org/10.1038/aps.2017.198 PMID: 29620049
15. Aird KM, Zhang G, Li H, Tu Z, Bitler BG, Garipov A, et al. Suppression of nucleotide metabolism underlies the establishment and maintenance of oncogene-induced senescence. Cell Rep. 2013; 3(4):1252–65. https://doi.org/10.1016/j.celrep.2013.03.004 PMID: 23562156
16. Bartkova J, Rezaei N, Liontos M, Karakaidos P, Kletsas D, Issaeva N, et al. Oncogene-induced senescence is part of the tumorigenesis barrier imposed by DNA damage checkpoints. Nature. 2006; 444 (7119):633–7. https://doi.org/10.1038/nature05268 PMID: 17136093
17. Pylayeva-Gupta Y, Grabocka E, Bar-Sagi D. RAS oncogenes: weaving a tumorigenic web. Nat Rev Cancer. 2011; 11(11):761–74. https://doi.org/10.1038/nrc3106 PMID: 21993244
18. Kotsantis P, Silva LM, Irmscher S, Jones RM, Folkes L, Gromak N, et al. Increased global transcription activity as a mechanism of replication stress in cancer. Nat Commun. 2016; 7:13087. https://doi.org/10.1038/ncomms13087 PMID: 27725641

19. Miron K, Golan-Lev T, Dvir R, Ben-David E, Kerem B. Oncogenes create a unique landscape of fragile sites. Nat Commun. 2015; 6:7094. https://doi.org/10.1038/ncomms8094 PMID: 25959793

20. Ogrunc M, Di Micco R, Liontos M, Bombardelli L, Mione M, Fumagalli M, et al. Oncogene-induced reactive oxygen species fuel hyperproliferation and DNA damage response activation. Cell Death Differ. 2014; 21(6):998–1012. https://doi.org/10.1038/cdd.2014.16 PMID: 24583638

21. Kimmelman AC. Metabolic Dependencies in RAS-Driven Cancers. Clin Cancer Res. 2015; 21(8):1828–34. https://doi.org/10.1158/1078-0432.CCR-14-2425 PMID: 25878364

22. Mannava S, Moparthy KC, Wheeler LJ, Natarajan V, Zucker SN, Fink EE, et al. Depletion of deoxyribonucleotide pools is an endogenous source of DNA damage in cells undergoing oncogene-induced senescence. Am J Pathol. 2013; 182(1):142–51. https://doi.org/10.1016/j.ajpath.2012.09.011 PMID: 23245831

23. Barnes R, Eckert K. Maintenance of Genome Integrity: How Mammalian Cells Orchestrate Genome Duplication by Coordinating Replicative and Specialized DNA Polymerases. Genes (Basel). 2017; 8(1). https://doi.org/10.3390/genes8010019 PMID: 28067843

24. Lujan SA, Williams JS, Kunkel TA. Eukaryotic genome instability in light of asymmetric DNA replication. Crit Rev Biochem Mol Biol. 2016; 51(1):43–52. https://doi.org/10.3109/10409238.2015.1117055 PMID: 26822554

25. Gao Y, Mutter-Rottmayer E, Zlatanou A, Vaziri C, Yang Y. Mechanisms of Post-Replication DNA Repair. Genes (Basel). 2017; 8(2). https://doi.org/10.3390/genes8020064 PMID: 28208741

26. Betous R, Rey L, Wang G, Pillaire MJ, Puget N, Selves J, et al. Role of TLS DNA polymerases eta and kappa in processing naturally occurring structured DNA in human cells. Mol Carcinog. 2009; 48(4):369–78. https://doi.org/10.1002/mc.20509 PMID: 19117014

27. Rey L, Sidorova JM, Puget N, Boudsocq F, Biard DS, Monnat RJ Jr., et al. Human DNA polymerase eta is required for common fragile site stability during unperturbed DNA replication. Mol Cell Biol. 2009; 29 (12):3344–54. https://doi.org/10.1128/MCB.00115-09 PMID: 19380493

28. Tsao WC, Eckert KA. Detours to Replication: Functions of Specialized DNA Polymerases during Oncogene-induced Replication Stress. Int J Mol Sci. 2018; 19(10). https://doi.org/10.3390/ijms19103255 PMID: 30347795

29. Tonzi P, Huang TT. Role of Y-family translesion DNA polymerases in replication stress: Implications for new cancer therapeutic targets. DNA Repair (Amst). 2019; 78:20–6. https://doi.org/10.1016/j.dnarep.2019.03.016 PMID: 30954011

30. Barnes RP, Hile SE, Lee MY, Eckert KA. DNA polymerases eta and kappa exchange with the polymerase delta holoenzyme to complete common fragile site synthesis. DNA Repair (Amst). 2017; 57:1–11. https://doi.org/10.1016/j.dnarep.2017.05.006 PMID: 28605669

31. Barnes RP, Tsao W, Moldovan G, Eckert K. DNA Polymerase Eta Prevents Tumor Cell Cycle Arrest and Cell Death During Recovery from Replication Stress. Cancer Research. 2018. https://doi.org/10.1158/0008-5472.CAN-17-3931 PMID: 30297532

32. Srivastava AK, Han C, Zhao R, Cui T, Dai Y, Mao C, et al. Enhanced expression of DNA polymerase eta contributes to cisplatin resistance of ovarian cancer stem cells. Proc Natl Acad Sci U S A. 2015; 112 (14):4411–6. https://doi.org/10.1073/pnas.1421365112 PMID: 25831546

33. Ceppi P, Novello S, Cambieri A, Longo M, Monica V, Lo Iacono M, et al. Polymerase eta mRNA expression predicts survival of non-small cell lung cancer patients treated with platinum-based chemotherapy. Clin Cancer Res. 2009; 15(3):1039–45. https://doi.org/10.1158/1078-0432.CCR-08-1227 PMID: 19188177

34. Costantino L, Sotiriou SK, Rantala JK, Magin S, Mladenov E, Helleday T, et al. Break-induced replication repair of damaged forks induces genomic duplications in human cells. Science. 2014; 343 (6166):88–91. https://doi.org/10.1126/science.1243211 PMID: 24310611

35. Yang Y, Gao Y, Mutter-Rottmayer L, Zlatanou A, Durando M, Ding W, et al. DNA repair factor RAD18 and DNA polymerase Polκ confer tolerance of oncogenic DNA replication stress. J Cell Biol. 2017; 216 (10):3097–115. https://doi.org/10.1083/jcb.201702006 PMID: 28835467

36. Kurashima K, Sekimoto T, Oda T, Kawabata T, Hanaoka F, Yamashita T. Polη, a Y-family translesion synthesis polymerase, promotes cellular tolerance of Myc-induced replication stress. J Cell Sci. 2018;131(12). https://doi.org/10.1242/jcs.212183 PMID: 29777036

37. Miller L. Analyzing western blots with Image Studio Lite 2013 [updated February 2, 2013. https://lukemiller.org/index.php/2013/02/analyzing-western-blots-with-image-studio-lite/.

38. Buj R, Chen CW, Dahl ES, Leon KE, Kuskovsky R, Maglakelidze N, et al. Suppression of p16 Induces mTORC1-Mediated Nucleotide Metabolic Reprogramming. Cell Rep. 2019; 28(8):1971–80.e8. https://doi.org/10.1016/j.celrep.2019.07.084 PMID: 31433975

39. Sidorova JM, Li N, Schwartz DC, Folch A, Monnat RJ. Microfluidic-assisted analysis of replicating DNA molecules. Nat Protoc. 2009; 4(6):849–61. https://doi.org/10.1038/nprot.2009.54 PMID: 19444242

40. Kehrli K, Phelps M, Lazarchuk P, Chen E, Monnat R Jr., Sidorova JM. Class I Histone Deacetylase HDAC1 and WRN RECQ Helicase Contribute Additively to Protect Replication Forks upon Hydroxyurea-induced Arrest. J Biol Chem. 2016; 291(47):24487–503. https://doi.org/10.1074/jbc.M115.708594 PMID: 27672210

41. Ghesquiere P, Elsherbiny A, Fortier E, McQuaid M, Mazzaferri J, Belanger F, et al. An open-source algorithm for rapid unbiased determination of DNA fiber length. DNA Repair (Amst). 2019; 74:26–37. https://doi.org/10.1016/j.dnarep.2019.01.003 PMID: 30665830

42. Tu Z, Aird KM, Bitler BG, Nicodemus JP, Beeharry N, Xia B, et al. Oncogenic RAS regulates BRIP1 expression to induce dissociation of BRCA1 from chromatin, inhibit DNA repair, and promote senescence. Dev Cell. 2011; 21(6):1077–91. https://doi.org/10.1016/j.devcel.2011.10.010 PMID: 22137763

43. Hayflick L, Moorhead PS. The serial cultivation of human diploid cell strains. Exp Cell Res. 1961; 25:585–621. https://doi.org/10.1016/0014-4827(61)90192-6 PMID: 13905658

44. Martin-Ruiz C, Saretzki G, Petrie J, Ladhoff J, Jeyapalan J, Wei W, et al. Stochastic variation in telomere shortening rate causes heterogeneity of human fibroblast replicative life span. J Biol Chem. 2004; 279(17):17826–33. https://doi.org/10.1074/jbc.M311980200 PMID: 14963037

45. Kohsaka S, Sasai K, Takahashi K, Akagi T, Tanino M, Kimura T, et al. A population of BJ fibroblasts escaped from Ras-induced senescence susceptible to transformation. Biochem Biophys Res Commun. 2011; 410(4):878–84. https://doi.org/10.1016/j.bbrc.2011.06.082 PMID: 21703241

46. Bertoletti F, Cea V, Liang CC, Lanati T, Maffia A, Avarello MDM, et al. Phosphorylation regulates human poleta stability and damage bypass throughout the cell cycle. Nucleic Acids Res. 2017; 45 (16):9441–54. https://doi.org/10.1093/nar/gkx619 PMID: 28934491

47. Hendriks IA, D'Souza RC, Yang B, Verlaan-de Vries M, Mann M, Vertegaal AC. Uncovering global SUMOylation signaling networks in a site-specific manner. Nat Struct Mol Biol. 2014; 21(10):927–36. https://doi.org/10.1038/nsmb.2890 PMID: 25218447

48. Serrano M, Lin AW, McCurrach ME, Beach D, Lowe SW. Oncogenic ras provokes premature cell senescence associated with accumulation of p53 and p16INK4a. Cell. 1997; 88(5):593–602. https://doi.org/10.1016/s0092-8674(00)81902-9 PMID: 9054499

49. Collado M, Gil J, Efeyan A, Guerra C, Schuhmacher AJ, Barradas M, et al. Tumour biology: senescence in premalignant tumours. Nature. 2005; 436(7051):642. https://doi.org/10.1038/436642a PMID: 16079833

50. Rayess H, Wang MB, Srivatsan ES. Cellular senescence and tumor suppressor gene p16. Int J Cancer. 2012; 130(8):1715–25. https://doi.org/10.1002/ijc.27316 PMID: 22025288

51. Chen YW, Harris RA, Hatahet Z, Chou KM. Ablation of XP-V gene causes adipose tissue senescence and metabolic abnormalities. Proc Natl Acad Sci U S A. 2015; 112(33):E4556–64. https://doi.org/10.1073/pnas.1506954112 PMID: 26240351

52. Garcia-Exposito L, Bournique E, Bergoglio V, Bose A, Barroso-Gonzalez J, Zhang S, et al. Proteomic Profiling Reveals a Specific Role for Translesion DNA Polymerase η in the Alternative Lengthening of Telomeres. Cell Rep. 2016; 17(7):1858–71. https://doi.org/10.1016/j.celrep.2016.10.048 PMID: 27829156

53. Tomicic MT, Aasland D, Naumann SC, Meise R, Barckhausen C, Kaina B, et al. Translesion polymerase eta is upregulated by cancer therapeutics and confers anticancer drug resistance. Cancer Res. 2014; 74(19):5585–96. https://doi.org/10.1158/0008-5472.CAN-14-0953 PMID: 25125662

54. Zhou W, Chen YW, Liu X, Chu P, Loria S, Wang Y, et al. Expression of DNA translesion synthesis polymerase eta in head and neck squamous cell cancer predicts resistance to gemcitabine and cisplatin-based chemotherapy. PLoS One. 2013; 8(12):e83978. https://doi.org/10.1371/journal.pone.0083978 PMID: 24376779

55. Volpe JP, Cleaver JE. Xeroderma pigmentosum variant cells are resistant to immortalization. Mutat Res. 1995; 337(2):111–7. https://doi.org/10.1016/0921-8777(95)00015-c PMID: 7565859

56. Kannouche P, Broughton BC, Volker M, Hanaoka F, Mullenders LH, Lehmann AR. Domain structure, localization, and function of DNA polymerase eta, defective in xeroderma pigmentosum variant cells. Genes Dev. 2001; 15(2):158–72. https://doi.org/10.1101/gad.187501 PMID: 11157773

57. Gabai VL, O'Callaghan-Sunol C, Meng L, Sherman MY, Yaglom J. Triggering senescence programs suppresses Chk1 kinase and sensitizes cells to genotoxic stresses. Cancer Res. 2008; 68(6):1834–42. https://doi.org/10.1158/0008-5472.CAN-07-5656 PMID: 18339864

58. Zhang YW, Otterness DM, Chiang GG, Xie W, Liu YC, Mercurio F, et al. Genotoxic stress targets human Chk1 for degradation by the ubiquitin-proteasome pathway. Mol Cell. 2005; 19(5):607–18. https://doi.org/10.1016/j.molcel.2005.07.019 PMID: 16137618

59. Park C, Suh Y, Cuervo AM. Regulated degradation of Chk1 by chaperone-mediated autophagy in response to DNA damage. Nat Commun. 2015; 6:6823. https://doi.org/10.1038/ncomms7823 PMID: 25880015

60. Kim AJ, Kim HJ, Jee HJ, Song N, Kim M, Bae YS, et al. Glucose deprivation is associated with Chk1 degradation through the ubiquitin-proteasome pathway and effective checkpoint response to replication blocks. Biochim Biophys Acta. 2011; 1813(6):1230–8. https://doi.org/10.1016/j.bbamcr.2011.03.012 PMID: 21440578

61. Zhang YW, Brognard J, Coughlin C, You Z, Dolled-Filhart M, Aslanian A, et al. The F box protein Fbx6 regulates Chk1 stability and cellular sensitivity to replication stress. Mol Cell. 2009; 35(4):442–53. https://doi.org/10.1016/j.molcel.2009.06.030 PMID: 19716789

62. Maya-Mendoza A, Ostrakova J, Kosar M, Hall A, Duskova P, Mistrik M, et al. Myc and Ras oncogenes engage different energy metabolism programs and evoke distinct patterns of oxidative and DNA replication stress. Mol Oncol. 2015; 9(3):601–16. https://doi.org/10.1016/j.molonc.2014.11.001 PMID: 25435281

63. Aguilera A, Garcia-Muse T. R loops: from transcription byproducts to threats to genome stability. Mol Cell. 2012; 46(2):115–24. https://doi.org/10.1016/j.molcel.2012.04.009 PMID: 22541554

64. Lewis JS, Spenkelink LM, Schauer GD, Yurieva O, Mueller SH, Natarajan V, et al. Tunability of DNA Polymerase Stability during Eukaryotic DNA Replication. Mol Cell. 2020; 77(1):17–25.e5. https://doi.org/10.1016/j.molcel.2019.10.005 PMID: 31704183

65. Boldinova EO, Wanrooij PH, Shilkin ES, Wanrooij S, Makarova AV. DNA Damage Tolerance by Eukaryotic DNA Polymerase and Primase PrimPol. Int J Mol Sci. 2017; 18(7). https://doi.org/10.3390/ijms18071584 PMID: 28754021

66. Mouron S, Rodriguez-Acebes S, Martinez-Jimenez MI, Garcia-Gomez S, Chocron S, Blanco L, et al. Repriming of DNA synthesis at stalled replication forks by human PrimPol. Nat Struct Mol Biol. 2013; 20(12):1383–9. https://doi.org/10.1038/nsmb.2719 PMID: 24240614

67. Rudd SG, Bianchi J, Doherty AJ. PrimPol-A new polymerase on the block. Mol Cell Oncol. 2014; 1(2):e960754. https://doi.org/10.4161/23723548.2014.960754 PMID: 27308331

68. Wan L, Lou J, Xia Y, Su B, Liu T, Cui J, et al. hPrimpol1/CCDC111 is a human DNA primase-polymerase required for the maintenance of genome integrity. EMBO Rep. 2013; 14(12):1104–12. https://doi.org/10.1038/embor.2013.159 PMID: 24126761

69. Yan S, Michael WM. TopBP1 and DNA polymerase-alpha directly recruit the 9-1-1 complex to stalled DNA replication forks. J Cell Biol. 2009; 184(6):793–804. https://doi.org/10.1083/jcb.200810185 PMID: 19289795

70. Bétous R, Pillaire MJ, Pierini L, van der Laan S, Recolin B, Ohl-Séguy E, et al. DNA polymerase κ-dependent DNA synthesis at stalled replication forks is important for CHK1 activation. EMBO J. 2013; 32(15):2172–85. https://doi.org/10.1038/emboj.2013.148 PMID: 23799366

71. Deschenes-Simard X, Gaumont-Leclerc MF, Bourdeau V, Lessard F, Moiseeva O, Forest V, et al. Tumor suppressor activity of the ERK/MAPK pathway by promoting selective protein degradation. Genes Dev. 2013; 27(8):900–15. https://doi.org/10.1101/gad.203984.112 PMID: 23599344

72. Barkley LR, Palle K, Durando M, Day TA, Gurkar A, Kakusho N, et al. c-Jun N-terminal kinase-mediated Rad18 phosphorylation facilitates Poleta recruitment to stalled replication forks. Mol Biol Cell. 2012; 23(10):1943–54. https://doi.org/10.1091/mbc.E11-10-0829 PMID: 22456510

73. Bienko M, Green CM, Sabbioneda S, Crosetto N, Matic I, Hibbert RG, et al. Regulation of translesion synthesis DNA polymerase eta by monoubiquitination. Mol Cell. 2010; 37(3):396–407. https://doi.org/10.1016/j.molcel.2009.12.039 PMID: 20159558

74. Despras E, Sittewelle M, Pouvelle C, Delrieu N, Cordonnier AM, Kannouche PL. Rad18-dependent SUMOylation of human specialized DNA polymerase eta is required to prevent under-replicated DNA. Nat Commun. 2016; 7:13326. https://doi.org/10.1038/ncomms13326 PMID: 27811911

75. Guerillon C, Smedegaard S, Hendriks IA, Nielsen ML, Mailand N. Multi-site SUMOylation restrains DNA polymerase eta interactions with DNA damage sites. J Biol Chem. 2020.

76. Tonzi P, Yin Y, Lee CWT, Rothenberg E, Huang TT. Translesion polymerase kappa-dependent DNA synthesis underlies replication fork recovery. Elife. 2018; 7. https://doi.org/10.7554/eLife.41426 PMID: 30422114

77. Roseaulin LC, Noguchi C, Martinez E, Ziegler MA, Toda T, Noguchi E. Coordinated degradation of replisome components ensures genome stability upon replication stress in the absence of the replication fork protection complex. PLoS Genet. 2013; 9(1):e1003213. https://doi.org/10.1371/journal.pgen.1003213 PMID: 23349636

78. Zheng DQ, Petes TD. Genome Instability Induced by Low Levels of Replicative DNA Polymerases in Yeast. Genes (Basel). 2018; 9(11). https://doi.org/10.3390/genes9110539 PMID: 30405078

79. Zhou Y, Meng X, Zhang S, Lee EY, Lee MY. Characterization of human DNA polymerase delta and its subassemblies reconstituted by expression in the MultiBac system. PLoS One. 2012; 7(6):e39156. https://doi.org/10.1371/journal.pone.0039156 PMID: 22723953

80. Dilley RL, Verma P, Cho NW, Winters HD, Wondisford AR, Greenberg RA. Break-induced telomere synthesis underlies alternative telomere maintenance. Nature. 2016; 539(7627):54–8. https://doi.org/10.1038/nature20099 PMID: 27760120

81. Minocherhomji S, Ying S, Bjerregaard VA, Bursomanno S, Aleliunaite A, Wu W, et al. Replication stress activates DNA repair synthesis in mitosis. Nature. 2015; 528(7581):286–90. https://doi.org/10.1038/nature16139 PMID: 26633632

82. Walsh E, Wang X, Lee MY, Eckert KA. Mechanism of replicative DNA polymerase delta pausing and a potential role for DNA polymerase kappa in common fragile site replication. J Mol Biol. 2013; 425 (2):232–43. https://doi.org/10.1016/j.jmb.2012.11.016 PMID: 23174185

83. Bergoglio V, Boyer AS, Walsh E, Naim V, Legube G, Lee MY, et al. DNA synthesis by Pol eta promotes fragile site stability by preventing under-replicated DNA in mitosis. J Cell Biol. 2013; 201(3):395–408. https://doi.org/10.1083/jcb.201207066 PMID: 23609533

84. Temprine K, Campbell NR, Huang R, Langdon EM, Simon-Vermot T, Mehta K, et al. Regulation of the error-prone DNA polymerase Polkappa by oncogenic signaling and its contribution to drug resistance. Sci Signal. 2020; 13(629). https://doi.org/10.1126/scisignal.aau1453 PMID: 32345725